

Human-Like Walking using Toes Joint and Straight Stance Leg

Sven Behnke, *Member, IEEE*

Albert-Ludwigs-Universität Freiburg, Computer Science Institute
Georges-Köhler-Allee 52, 79110 Freiburg, Germany
behnke@informatik.uni-freiburg.de

Abstract—This paper describes the use of an actuated toes joint in a humanoid robot to achieve human-like bipedal walking. The robot does not shorten the stance leg, but uses the segment between the ankle joint and the toes joint to over-extend the unloading leg in the double-support phase.

Experiments with the servo-based humanoid robot Toni show that this approach leads to low energy-consumption in the knees and allows walking dynamically with large steps.

Index Terms—Humanoid robot, bipedal walking, toes joint.

I. INTRODUCTION

THE importance of toes joints for bipedal walking has been investigated by several researchers. For instance, Hirai [1] states that toes joints are not necessary for bipedal walking. Consequently, almost all humanoid robots have been constructed with a non-actuated foot-plate. Honda Asimo [2] and Johnnie [3] are examples for bipedal robots that walk without toes joints.

In order to shift the weight from the unloading leg to the loading leg in the double-support phase, the length of the loading leg must be shortened relative to the unloading leg. When walking with large steps, most humanoid robots shorten the loading leg by bending its knee, because the unloading leg is in this situation already fully extended. This approach leads to the bipedal walking with bent stance legs that is typical for today's humanoid robots. This walk does not only look unnatural, it also leads to high torques in the knee, hip, and ankle joints of the stance leg. Consequently, high-power actuators are needed and energy consumption is high as well.

Humans walk in a different way. They do not shorten the loading leg, but over-extend the unloading leg. This is achieved by bending the foot while standing on the toes. The segment between the ankle joint and the toes joint provides the extra leg length needed to shift the weight. The over-extension of the unloading leg allows for a straight stance leg, and hence for energy-efficient walking. We applied this observation to the design and the control of the humanoid robot Toni.

This paper is organized as follows. In the next section, we review some of the related work. Section III describes Toni's mechanical and Section IV its electrical design in detail.

Section V describes how Toni is controlled to achieve human-like walking with toes joint and straight stance leg. Section VI summarizes experimental results obtained with this gait.

II. RELATED WORK

Humanoid robots have become a very popular research tool. Their anthropomorphic body shape is helpful for acting in environments that have been designed for humans, in particular for the interaction with people. In addition to speech, a humanoid robot can try to use the same means for intuitive multimodal communication that people use: body language, gestures, mimics, and gaze. Consequently, a number of research groups, especially in Japan, are constructing humanoid robots. A list of projects is maintained by Willis [4].

Only few researchers have investigated the use of toes joints for bipedal robots. Kumagai and Emura [5] proposed the use of passive toes joints in order to achieve stable foot lifting. Koganezawa and Osamu [6] describe a robot with joints that can be used both in an active and a passive mode. They propose the use of toes joints to decrease energy consumption while walking. Active toes joints have also been proposed to step-up stairs [7], [8].

To our knowledge, only the H6/7 robots of Tokyo University possess active toes joints. Nishiwaki et al. [9] describe their use to reduce maximal knee-joint speed while walking, to increase the step height when climbing, and to knee down with limited knee-joint angle.

In addition to the expensive larger humanoid robots, which are usually driven by DC-motors and harmonic drive gears, some smaller servo-driven humanoid robots have been developed recently [10], [11], [12]. Servo motors are used for humanoid robots because of their low cost and because of their good weight-to-torque ratio. The servo-driven robots have up to 22DOFs and a size of 30-40cm. None of these robots has toes joints.

III. MECHANICAL DESIGN

Fig. 1 shows two views of our humanoid robot Toni, ready to kick the ball. It has been designed for the 2005 RoboCup Humanoid League competitions. As can be seen, Toni has human-like proportions and a slim appearance. Its mechanical design focused on weight reduction. Toni is 74cm tall and has a total weight of only 2.2kg.

The robot is driven by 18 servo motors: 6 per leg and 3 in each arm. The six leg-servos allow for flexible leg movements. Two orthogonal servos form the 2DOF hip joint and the 2DOF ankle joint. One servo drives the knee joint. Toni's active toes joint is located in the frontal part of the foot plate.

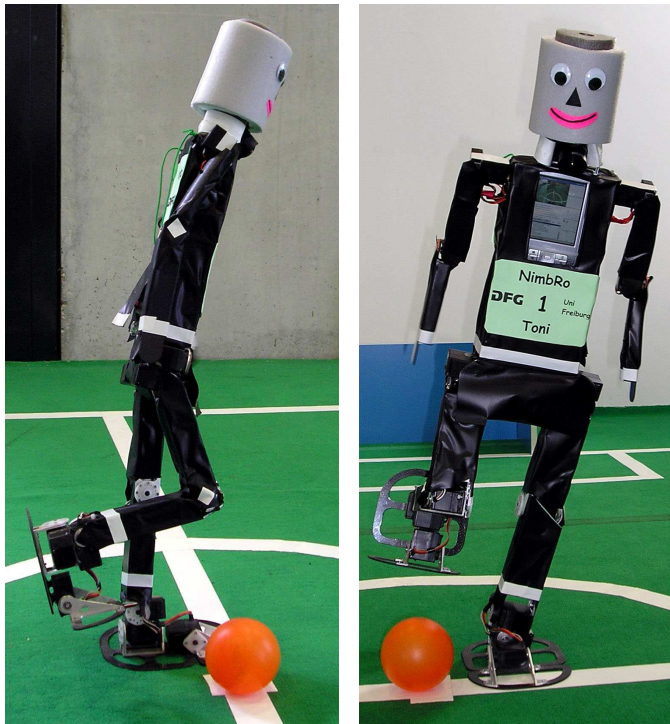


Fig. 1. Two views of the humanoid robot Toni, ready to kick.

We selected the S9192 servos from Futaba to drive the hips, the knees, and the ankles. These digital servos are rated for a torque of 200Ncm. They have a weight of only 85g. The toes joints need less torque. They are powered by JR 8511 servos (185Ncm, 66g). We augmented all servos by adding a ball bearing on their back, opposite to the driven axis. This made a stiff joint construction possible.

Toni's arms do not need to be as strong as the legs. They are powered by SES640 servos (64Ncm, 28g). Two orthogonal servos constitute the shoulder joint and one servo drives the elbow joint.

The skeleton of the robot is mostly constructed from aluminum extrusions with rectangular tube cross section. In order to reduce weight, we removed all material not necessary for stability. Toni's feet and its arms are made from sheets of carbon composite material. Its head is there for completeness only. It is made of lightweight foam.

IV. ELECTRONICS

Toni is fully autonomous. It is powered by high-current Lithium-polymer rechargeable batteries, which are located in the pelvis. Two Kokam 2000H cells last for about 30 minutes of operation. They can be discharged with 30A and have a weight of only 110g.

The servos are interfaced to three tiny ChipS12 microcontroller boards, shown in Fig. 2(a). One of these boards is

located in each thigh and one board is hidden in the pelvis. These boards feature the Motorola MC9S12C32 chip, a 16-bit controller belonging to the popular HCS12 family. We clock it with 24MHz. It has 2kB RAM, 32kB flash, a RS232 serial interface, CAN bus, 8 timers, 5 PWM channels, and 8 A/D converters. We use the timer module to generate pulses of 1...2ms duration at a rate of 180Hz in hardware. These pulses encode the target positions for the servos. Up to eight servos can be controlled with one board.

In order to keep track of the actual servo movements, we interfaced their potentiometers to the A/D converters of the HCS12. By analyzing the temporal fine structure of these signals, we estimate not only the current servo positions, but also the PWM duty cycles of their motors.

In addition to these joint sensors, Toni is equipped with an attitude sensor, shown in Fig. 2(b). It consists of a dual-axis accelerometer (Analog Devices ADXL203, $\pm 1.5g$) and two gyroscopes (ADXRS 150/300, $\pm 150/300$ deg/s). This attitude sensor is located in its pelvis. The four analog sensor signals are digitized with A/D converters of the HCS12 and are preprocessed by the microcontroller.

The microcontrollers communicate with each other via a CAN bus at 1MBaud and with a main computer via a RS232 serial line at 115KBaud.

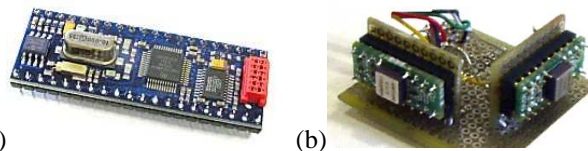


Fig. 2. Electronics: (a) ChipS12 microcontroller board featuring HCS12C32; (b) Attitude sensor consisting of a dual-axis accelerometer and two gyroscopes.

Every 12ms, target positions for the servos are sent from the main computer to the HCS12 boards, which generate intermediate targets at 180Hz. This yields smooth joint movements. The microcontrollers send the preprocessed sensor readings back. This allows keeping track of the robot's state in the main computer.

We use a Pocket PC as main computer, which is located in Toni's chest (see Fig. 1). The model FSC Pocket Loox 720 has a weight of only 170g, including the battery. It features a 520MHz XScale processor PXA-272, 128MB RAM, 64MB flash memory, a touch-sensitive display with VGA resolution, Bluetooth, wireless LAN, a RS232 serial interface, and an integrated 1.3 Mpixel camera.

This computer runs behavior control, computer vision, and wireless communication. It is equipped with a Lifeview Fly-CAM CF 1.3M that has been fitted to an ultra-wide-angle lens. The lens is located approximately at the position of the larynx. The wide field of view of this camera (vertically about 112°) allows Toni to see at the same time its own feet and objects above the horizon. The horizontal field of view is approximately 150° .

V. BEHAVIOR CONTROL

We control Toni using a framework that supports a hierarchy of reactive behaviors [13]. This framework allows for structured behavior engineering. Multiple layers that run on different time scales contain behaviors of different complexity. This framework forces the behavior engineers to define abstract sensors that are aggregated from faster, more basic sensors. Abstract actuators give higher-level behaviors the possibility to configure lower layers in order to eventually influence the state of the world.

The framework also supports an agent hierarchy. For Toni we use three levels of this hierarchy: individual joint, body part, and entire robot. This structure restricts interactions between the system variables and thus reduces the complexity of behavior engineering.

The lowest level of this hierarchy, the control loop within the servo, has been implemented by the servo manufacturer. It runs at about 300Hz for the digital servos. We monitor target positions, actual positions, and motor duties.

At the next layer, we generate target positions for the individual joints of a body-part at a rate of 83.3Hz. We make sure that the joint angles vary smoothly. Furthermore, the targets are smoothed in the HCS12 boards at 180Hz. This layer implements an interface that describes the behavior of body parts.

A. Leg Interface

The entire leg can be positioned relative to the trunk using leg extension (the distance from the hip joint to the ankle joint), leg angle (angle between the pelvis plate and the line from hip to ankle), and foot angle (angle between foot plate and pelvis plate).

Let $\theta_{\text{Leg}} = (\theta_{\text{Leg}}^1, \theta_{\text{Leg}}^s)$ denote the desired leg angle with the convention that the sagittal leg angle $\theta_{\text{Leg}}^s = 0$ if the leg is parallel to the trunk and $\theta_{\text{Leg}}^s > 0$ if the leg is in front of the trunk. Similarly, $\theta_{\text{Leg}}^1 = 0$ if the leg is parallel to the trunk, and $\theta_{\text{Leg}}^1 > 0$ if the leg is moved outwards in the lateral plane. Furthermore, $\theta_{\text{Foot}} = (\theta_{\text{Foot}}^1, \theta_{\text{Foot}}^s)$ denotes the desired foot angle, $\theta_{\text{Foot}} = (0, 0)$ if the foot is parallel to the pelvis plate. Finally, $-1 \leq \gamma \leq 0$ denotes the desired leg extension, with the convention that $\gamma = 0$ if the leg is fully extended and $\gamma = -1$ if the leg is shortened to $\eta_{\text{min}} = 0.875$ of its original length.

Now, the target relative leg length η can be computed as $\eta = 1 + (1 - \eta_{\text{min}})\gamma$. The knee angle

$$\theta_{\text{Knee}} = -2 \cdot \arccos(\eta) \quad (1)$$

shortens the leg, but would also change the leg and foot angles. Because the thigh and shank of the robot have the same length, we can subtract $0.5 \cdot \theta_{\text{Knee}}$ from θ_{Hip}^s and from θ_{Ankle}^s to compensate this effect. The desired leg angle θ_{Leg} is added to the θ_{Hip} and subtracted from θ_{Ankle} to keep the foot angle unchanged. Finally, the foot angle θ_{Foot} is added to θ_{Ankle} . This yields:

$$\theta_{\text{Hip}} = \theta_{\text{Leg}} - (0, 0.5 \cdot \theta_{\text{Knee}}) \quad (2)$$

$$\theta_{\text{Ankle}} = \theta_{\text{Foot}} - \theta_{\text{Leg}} - (0, 0.5 \cdot \theta_{\text{Knee}}) \quad (3)$$

The leg interface represented by $\theta_{\text{Leg}}, \theta_{\text{Foot}}$, and γ is a more abstract actuator space than the space spanned by the individual joint angles $\theta_{\text{Hip}} = (\theta_{\text{Hip}}^1, \theta_{\text{Hip}}^s), \theta_{\text{Knee}}$, and $\theta_{\text{Ankle}} = (\theta_{\text{Ankle}}^1, \theta_{\text{Ankle}}^s)$. It simplifies the implementation of dynamic walking, because its dimensions are less dependant than the individual joints angles. By changing only one target, e.g. the target leg extension γ , multiple joints are actuated in a coordinated way.

B. Central Clock

A central clock $-\pi \leq \phi_{\text{Trunk}} < \pi$ running in the trunk determines the step frequency. Both legs derive their own gait phase $-\pi \leq \phi_{\text{Leg}} < \pi$ by shifting the trunk phase by $\pm\pi/2$. Based on its gait phase, each leg generates trajectories for its leg extension, leg angle, foot angle, and toes joint angle θ_{Toe} . The convention is that $\theta_{\text{Toe}} = 0$ if the foot plate is even, and $\theta_{\text{Toe}} > 0$ if the frontal part of the foot plate is tilted upwards, relative to the rear part of the foot plate.

C. Dynamic Walking

The two key ingredients for generating dynamic walking are lateral shifting of the robot's center of mass, and movement of the legs in walking direction. The swinging leg is shortened while it is moved quickly into the walking direction. At the same time, the supporting leg has maximal extension and is moved slowly against the walking direction.

- **Shifting:** The shifting of the robot's center of mass is done in a sinusoidal way:

$$\theta_{\text{Shift}} = a_{\text{Shift}} \cdot \sin(\phi_{\text{Leg}}), \quad (4)$$

Where $a_{\text{Shift}} = 0.09$ is the shifting amplitude. Both, the lateral leg and foot angles are used to shift the robot:

$$\theta_{\text{LegShift}} = \begin{cases} \theta_{\text{Shift}} & \text{if } \phi_{\text{Leg}} \leq 0 \\ 2.0 \cdot \theta_{\text{Shift}} & \text{otherwise} \end{cases}, \quad (5)$$

$$\theta_{\text{FootShift}} = 0.75 \cdot \theta_{\text{Shift}}. \quad (6)$$

The leg angle moves more outwards than inwards, in order to prevent collisions between the legs.

- **Shortening:** As the robot swings to a side, the opposite leg is not needed to support the weight. It can be shortened. The time course of the shortening is determined by the shortening phase:

$$\phi_{\text{Short}} = v_{\text{Short}}(\phi_{\text{Leg}} + \pi/2 + o_{\text{Short}}), \quad (7)$$

where $v_{\text{Short}} = 2.75$ determines the duration of the shortening and $o_{\text{Short}} = -0.10$ determines the phase shift of the shortening relative to the lateral weight shifting. A cosine now produces smooth transitions between the fully extended leg and the shortened leg:

$$\gamma_{\text{Short}} = \begin{cases} -0.5(\cos(\phi_{\text{Short}}) + 1) & \text{if } -\pi \leq \phi_{\text{Short}} < \pi \\ 0 & \text{otherwise} \end{cases}. \quad (8)$$

- **Loading:** Immediately after the leg is fully extended and the heel landed, it is shortened a second time, in order to facilitate loading of this leg:

$$\phi_{\text{Load}} = v_{\text{Load}} \cdot \text{piCut}(\phi_{\text{Leg}} + \pi/2 - \pi / v_{\text{Short}} + o_{\text{Short}}) - \pi, \quad (9)$$

where $v_{\text{Load}} = 5$ determines the duration of the second shortening. The function $\text{piCut}(\cdot)$ maps its argument to the range $[-\pi, \pi)$ by adding multiples of 2π . The amplitude of the second shortening depends on the swing amplitude $a_{\text{Swing}} = 0.5$:

$$a_{\text{Load}} = 0.5 \cdot (1 - \cos(a_{\text{Swing}})). \quad (10)$$

It is also computed using a cosine:

$$\gamma_{\text{Load}} = \begin{cases} -0.5(\cos(\phi_{\text{Load}}) + 1) & \text{if } -\pi \leq \phi_{\text{Load}} < \pi \\ 0 & \text{otherwise} \end{cases}. \quad (11)$$

• **Swinging:** After the leg has been unloaded and shortened, it is moved quickly to the front. This swing is reversed slowly during the rest of the gait cycle. The time course of the swing is described by the swing phase:

$$\phi_{\text{Swing}} = v_{\text{Swing}}(\phi_{\text{Leg}} + \pi/2 + o_{\text{Swing}}), \quad (12)$$

where $v_{\text{Swing}} = 1.75$ is the swing speed and $o_{\text{Swing}} = -0.2$ is the phase shift of the swinging. While the swinging is sinusoidal, the reverse motion is linear:

$$\theta_{\text{Swing}} = \begin{cases} \sin(\phi_{\text{Swing}}) & \text{if } -\pi/2 \leq \phi_{\text{Swing}} < \pi/2 \\ b(\phi_{\text{Swing}} - \pi/2) - 1 & \text{if } \pi/2 \leq \phi_{\text{Swing}} \\ b(\phi_{\text{Swing}} + \pi/2) + 1 & \text{otherwise.} \end{cases} \quad (13)$$

The speed of the reverse motion is:

$$b = -(2/(2 \cdot \pi \cdot v_{\text{Swing}} - \pi)).$$

The swing is done with the sagittal leg angle and balanced partially with the sagittal foot angle:

$$\theta_{\text{LegSwing}} = a_{\text{Swing}} \cdot \theta_{\text{Swing}}, \quad (14)$$

$$\theta_{\text{FootSwing}} = 0.25 \cdot a_{\text{Swing}} \cdot \theta_{\text{Swing}}. \quad (15)$$

• **Over-Extension:** At the end of the stance phase, before the leg shortening, the unloading leg is over-extended using its toes joint in order to shift the weight to the other leg. The time course is described by the extension phase:

$$\phi_{\text{Ext}} = v_{\text{Ext}} \cdot \text{piCut}(\phi_{\text{Leg}} + \pi/2 + \pi/v_{\text{Short}} + o_{\text{Short}}), \quad (16)$$

where $v_{\text{Ext}} = 2.0$ determines the duration of the leg over-extension. The amplitude of the extension depends on the swing amplitude:

$$a_{\text{Ext}} = 5 \cdot (1 - \cos(a_{\text{Swing}})). \quad (17)$$

A cosine is used to produce a smooth over-extension:

$$\theta_{\text{Ext}} = \begin{cases} 0.5(\cos(\phi_{\text{Ext}}) + 1) & \text{if } -\pi \leq \phi_{\text{Ext}} < \pi \\ 0 & \text{otherwise} \end{cases}. \quad (18)$$

The frontal part of the foot plate is kept parallel to the ground:

$$\theta_{\text{FootExt}} = -a_{\text{Ext}} \cdot \theta_{\text{Ext}}, \quad (19)$$

$$\theta_{\text{ToesExt}} = a_{\text{Ext}} \cdot \theta_{\text{Ext}} - 0.25 \cdot a_{\text{Swing}} \cdot \theta_{\text{Swing}}. \quad (20)$$

The sagittal leg angle is corrected for the effect of the over-extension:

$$\theta_{\text{LegExt}} = -0.5 \cdot \text{asin}(0.25 \cdot \cos(\theta_{\text{ToesExt}})) - \text{asin}(0.25). \quad (21)$$

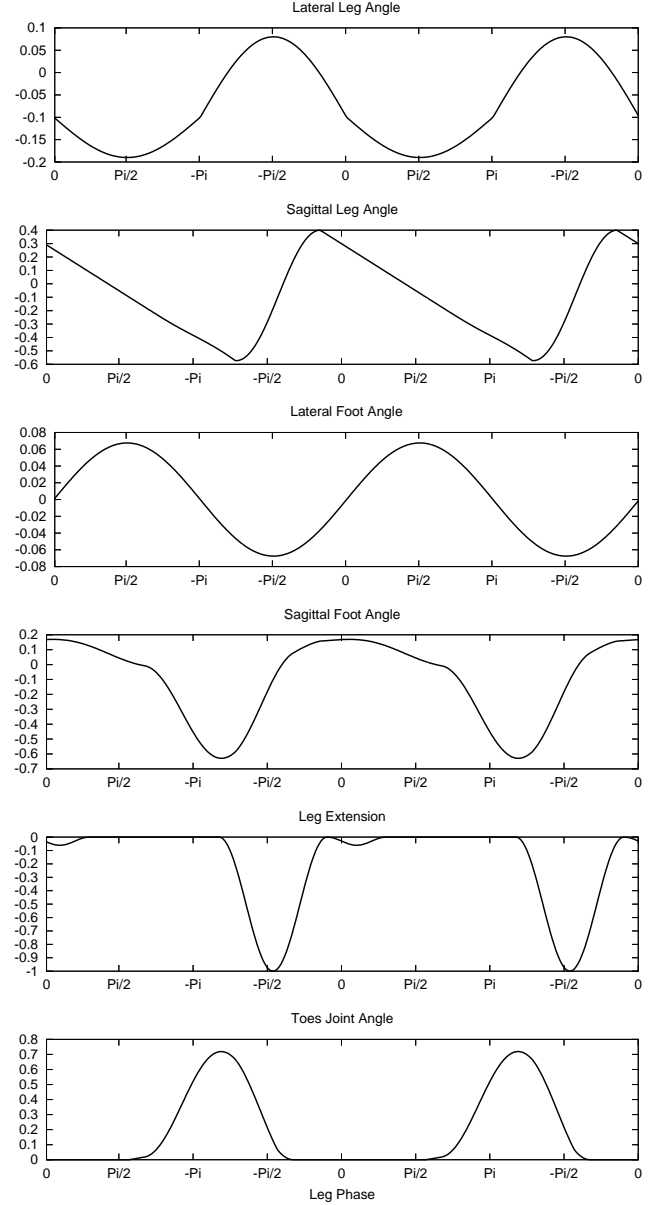


Fig. 3. Trajectories generating dynamic walking using toes joint and straight stance leg. See text for details.

• **Balance:** The robot is balanced by tilting it with every step in the sagittal plane and by adding offsets to the leg and foot angles:

$$\theta_{\text{FootBal}}^s = 0.05 + 0.08 \cdot a_{\text{Swing}} \cdot \sin(2 \cdot \phi_{\text{Leg}} + 0.5), \quad (22)$$

$$\theta_{\text{LegBal}}^l = -0.10, \quad (23)$$

$$\theta_{\text{LegBal}}^s = -0.10. \quad (24)$$

The negative lateral leg angle moves the feet closer together. The negative sagittal leg angle moves the robot forward. The negative sagittal foot angle tilts the robot forward.

• **Output:** The individual components of the walking motion are combined as follows:

$$\theta_{\text{Leg}}^l = \theta_{\text{LegShift}} + \theta_{\text{LegBal}}^l, \quad (25)$$

$$\theta_{\text{Leg}}^s = \theta_{\text{LegSwing}} + \theta_{\text{LegExt}} + \theta_{\text{LegBal}}^s, \quad (26)$$

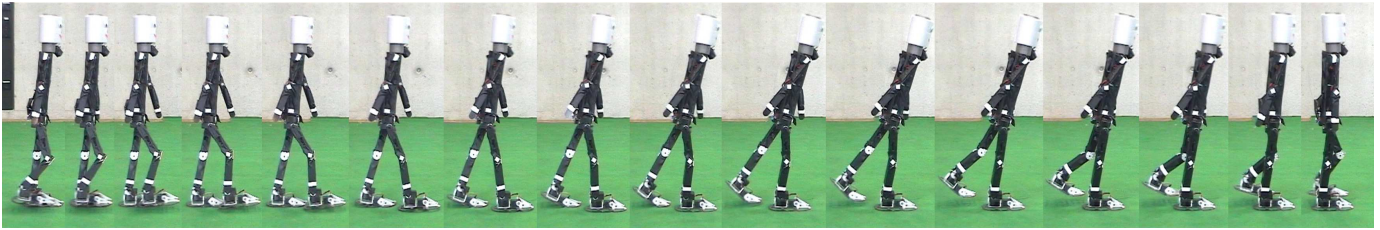


Fig. 6. Sequence of successive frames extracted from video showing an entire step of the walking robot (lateral view).

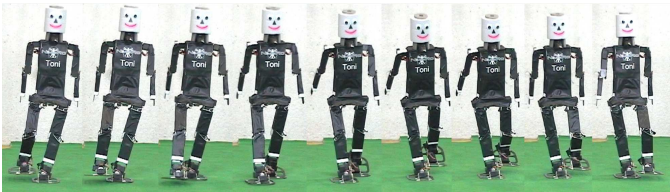


Fig. 4. Sequence of every other frame extracted from video showing an entire step of the walking robot (frontal view).

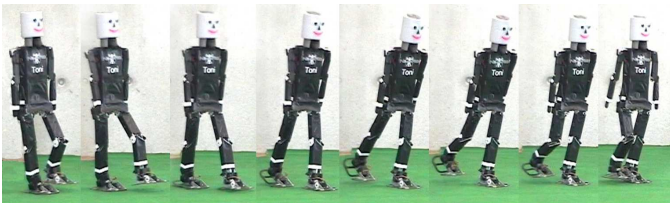


Fig. 5. Sequence of every other frame extracted from video showing an entire step of the walking robot (perspective view).

$$\theta_{\text{Foot}}^l = \theta_{\text{FootShift}}, \quad (27)$$

$$\theta_{\text{Foot}}^s = \theta_{\text{FootSwing}} + \theta_{\text{FootExt}} + \theta_{\text{FootBal}}^s, \quad (28)$$

$$\theta_{\text{Toes}}^l = \theta_{\text{ToesExt}}, \quad (29)$$

$$\gamma = \gamma_{\text{Short}} + \gamma_{\text{Load}}. \quad (30)$$

The resulting trajectories are depicted in Fig. 3. The arms of the robot are moved in a similar way. Each arm moves synchronously with its contralateral leg.

VI. RESULTS

Fig. 4, Fig. 5, and Fig. 6 show sequences of frontal, perspective, and lateral views of the walking robot, respectively. They have been extracted from a video which can be downloaded from http://www.nimbro.net/movies/toni/Toni_Walking_Human-like.wmv and which is also included in the proceedings CD.

It can be observed that Toni walks dynamically with relatively large steps. The robot stands on the frontal part of its foot plate, before lifting the foot. In this situation, the unloading leg is over-extended. In the stance phase, the supporting leg is fully extended. The swinging foot lands smoothly on the heel. The upper body of the robot translates laterally, but does not tilt much in the lateral plane. While the upper body is moved in forward direction, it tilts in the sagittal plane when the robot shifts its weight from one leg to the other.

An average step size of 20.6cm was measured. With the step frequency of 1.03Hz the resulting speed is 21.2cm/s. Energy

consumption in the joints can be estimated from the servo temperatures after walking longer distances. While the hip-servos had the highest temperature, the knee servos were cool and the ankle servos had an intermediate temperature. This indicates that the straight stance leg relieves the knee joint from high torques.

VII. CONCLUSIONS

This paper described the use of toes joints to achieve human-like walking for humanoid robots. We over-extend the unloading leg before toes-off and keep the stance leg of the robot straight. We implemented this gait for our 18DOF robot Toni. The resulting walking speed was 21.2cm/s, which is quite high, given Toni's size of 74cm.

In addition to human-like walking, we implemented omnidirectional walking, kicking, and basic soccer skills for Toni, which will be detailed elsewhere. We presented Toni for the first time to the public during the 21st Chaos Communication Congress (Berlin, Dec. 2004). At RoboCup German Open (April 2005), we showed penalty kick demonstrations. At RoboCup 2005 in Osaka, Japan, Toni will face the world's best humanoid soccer robots.

ACKNOWLEDGMENT

The author would like to thank the following students who contributed to Toni's development: Michael Schreiber, Thorsten Kramer, Tobias Langner, Jörg Stückler, Konstantin Welke, and Rui Zhou. Jürgen Müller helped to interface the camera and to establish wireless communication. The RoboCup team FU-Fighters provided the sources of a framework for implementing a hierarchy of reactive behaviors.

REFERENCES

- [1] K. Hirai, "Current and future perspective of honda humanoid robot," in *Proceedings of the IEEE/RSJ International Conference on Intelligent Robots and Systems (IROS'97)*, 1997, pp. 500–508.
- [2] Honda, "ASIMO. <http://world.honda.com/asimo>."
- [3] F. Pfeiffer, K. Löffler, and M. Gienger, "The concept of jogging johnnie," in *Proceedings of the 2002 IEEE International Conference on Robotics and Automation (ICRA'02)*, vol. 3, 2002, pp. 3129–3135.
- [4] C. Willis, "World's greatest android projects. <http://www.androidworld.com>."
- [5] M. Kumagai and T. Emura, "Sensor-based walking of human type biped robot that has 14 degree of freedoms," in *Proceedings of the 4th Annual Conference on Mechatronics and Machine Vision in Practice (M2VIP'97)*, 1997, p. 112.
- [6] K. Koganezawa and M. Osamu, "Active/passive hybrid walking by the biped robot TOKAI ROBO-HABILIS," in *Proceedings of the IEEE/RSJ International Conference on Intelligent Robots and Systems (IROS'02)*, 2002, p. #541.

- [7] W. Yabuki, J. Furusho, and A. Sano, "Basic study of dynamic walking control of biped robots on the gentle stairs," in *In Proceedings of 9th Annual Conference of Robotics Society of Japan*, 1991, pp. 319–320.
- [8] N. Kanamori, M. Sakaguchi, and J. Furusho, "Development of a biped robot with fourteen-degree of freedom," in *In Proceedings of '96 Annual Symposium of Robotics-Mechatronics*, 1996, pp. 295–296.
- [9] K. Nishiwaki, S. Kagami, Y. Kuniyoshi, M. Inaba, and H. Inoue, "Toe joints that enhance bipedal and fullbody motion of humanoid robots," in *Proceedings of the 2002 IEEE International Conference on Robotics and Automation (ICRA'02)*, 2002, pp. 3105–3110.
- [10] Kondo Kagaku Co., Ltd., "KHR-1. <http://www.kondo-robot.com>."
- [11] Vstone Co., Ltd., "<http://www.vstone.co.jp>."
- [12] C. Zhou and P. K. Yue, "Robo-Erectus: a low-cost autonomous humanoid soccer robot," *Advanced Robotics*, vol. 18, no. 7, pp. 717–720, 2004.
- [13] S. Behnke and R. Rojas, "A hierarchy of reactive behaviors handles complexity," in *Balancing Reactivity and Social Deliberation in Multi-Agent Systems*, M. Hannebauer, J. Wendler, and E. Pagello, Eds. Springer, 2001, pp. 125–136.



Sven Behnke studied Computer Science and Business Administration at Martin-Luther-Universität Halle-Wittenberg (and 1994/95 at University of Houston), from where he received his MS CS (Dipl.-Inform.) in 1997. Afterwards he moved to Freie Universität Berlin, where he received his PhD (Dr. rer. nat.) in Computer Science in 2002. During 2003, he worked as a postdoc at the International Computer Science Institute in Berkeley, CA. Since 2004, he heads the junior research group Humanoid Robots at Albert-Ludwigs Universität Freiburg. His

research interests include autonomous intelligent systems and neural information processing.